IVYSPRING INTERNATIONAL PUBLISHER

Theranostics

2018; 8(2): 575-592. doi: 10.7150/thno.21648

Research Paper

# circRNA Mediates Silica-Induced Macrophage Activation Via HECTD1/ZC3H12A-Dependent Ubiquitination

Zewei Zhou[1, 2, 3, 4], Rong Jiang[1], Xiyue Yang[1], Huifang Guo[1], Shencun Fang[5], Yingming Zhang[5], Yusi Cheng[1], Jing Wang[1], Honghong Yao[2, 4], and Jie Chao[1, 3, 4]✉

1. Department of Physiology, School of Medicine, Southeast University, Nanjing, Jiangsu, 210009, China;
2. Department of Pharmacology, School of Medicine, Southeast University, Nanjing, Jiangsu, 210009, China;
3. Department of Respiration, Zhongda Hospital, School of Medicine, Southeast University, Nanjing, Jiangsu 210009, China;
4. Key Laboratory of Developmental Genes and Human Disease, Southeast University, Nanjing, 210096, China;
5. Nine Department of Respiratory Medicine, Nanjing Chest Hospital, Nanjing, Jiangsu, 210029, China;
6. Department of Respiratory Medicine, Nanjing Drum Tower Hospital, Nanjing, Jiangsu, 210029, China;
7. Department of Respiratory Medicine, First Affiliated Hospital of Nanjing Medical University, Nanjing, Jiangsu 210029, China.

✉ Corresponding author: Jie Chao, Ph.D., Department of Physiology, School of Medicine, Southeast University, 87 Dingjiaqiao Rd, Nanjing, Jiangsu, 210009, China Phone: +86-25-83272312 Fax: +86-25-83272312 Email: chaojie@seu.edu.cn



Received: 2017.06.27; Accepted: 2017.10.12; Published: 2018.01.01

## Abstract

**Rationale:** Phagocytosis of silicon dioxide ($SiO_2$) into lung cells causes an inflammatory cascade that results in fibroblast proliferation and migration, followed by fibrosis. Circular RNAs (circRNAs) are a subclass of non-coding RNAs detected within mammalian cells; however, researchers have not determined whether circRNAs are involved in the pathophysiological process of silicosis. The upstream molecular mechanisms and functional effects on cell apoptosis, proliferation and migration were investigated to elucidate the role of circRNAs in $SiO_2$-induced inflammation in pulmonary macrophages.

**Methods:** Primary cultures of alveolar macrophages from healthy donors and patients as well as the RAW264.7 macrophage cell line were used to explore the functions of circHECTD1 (HECT domain E3 ubiquitin protein ligase 1) in macrophage activation.

**Results:** The results of the experiments indicated that 1) $SiO_2$ concomitantly decreased circHECTD1 levels and increased HECTD1 protein expression; 2) circHECTD1 and HECTD1 were involved in $SiO_2$-induced macrophage activation via ubiquitination; and 3) $SiO_2$-activated macrophages promoted fibroblast proliferation and migration via the circHECTD1/HECTD1 pathway. Tissue samples from silicosis patients confirmed the upregulation of HECTD1.

**Conclusions:** Our study elucidated a link between $SiO_2$-induced macrophage activation and the circHECTD1/HECTD1 pathway, thereby providing new insight into the potential use of HECTD1 in the development of novel therapeutic strategies for treating silicosis.

Key words: circHECTD1; migration; fibrosis; silicosis.

## Introduction

Silicosis is a type of occupational disease caused by long-term exposure to high levels of dust containing excess levels of free silica (crystalline silicon dioxide) from mining and other dusty occupational environments [1, 2]. Although preventive measures have been established for many decades, silicosis remains a potentially fatal, incurable and disabling pulmonary disease that is characterized by silicotic nodule formation and pulmonary interstitial fibrosis [3]. Silicosis occurs worldwide but is particularly prevalent in undeveloped countries due to poor surveillance [4]. Additionally, the incidence and prevalence of silicosis are increasing markedly, and effective therapies are not currently

available [5]. Despite the plethora of studies that have been conducted to investigate the toxicity of crystalline silica over the last several decades, the exact mechanism of silicosis currently remains elusive.

Circular RNAs (circRNAs) are a class of non-coding RNAs with a closed continuous loop structure in which the 3' and 5' ends are joined together and are known to be involved in disease processes [6-10]. Recently, circRNAs have been identified as competing endogenous RNAs (ceRNAs) that act as a sponge for miRNAs via complementary base paring. Therefore, the function of circRNAs is only beginning to be understood. The circRNA ciRS-7 is a recently identified human circRNA that acts as a sponge for miR-7 and is resistant to miRNA-mediated target destabilization; therefore, ciRS-7 strongly suppresses miR-7 activity [11]. Additionally, circRNAs affect gene transcription through their association with phosphorylated Pol II [12] or compete with pre-mRNA splicing [13]. These findings all lend strong support to the hypothesis that circRNAs play fundamental roles in various cellular processes.

The morbidity of silicosis shows inter-individual differences, which may be due to variations in individuals' inflammatory responses. Silicosis is initiated via the phagocytosis of silica particles by alveolar macrophages; these macrophages release various oxidants and cytokines, which play crucial roles in the development and progression of the disease [14]. Hence, investigations into the role of circRNAs in the progression and treatment of inflammation and fibrosis are needed.

In this study, the circHECTD1/HECTD1 pathway was shown to cause macrophage activation and death, and these effects subsequently induced fibroblast activation. These findings reveal a novel function of circRNAs in $SiO_2$-induced fibrosis and suggest that the circHECTD1/HECTD1 pathway might be involved in multiple steps of the fibrosis process.

## Materials and Methods

### Reagents

Silicon dioxide in which 80% of particles exhibited a diameter of less than 5 μm was purchased from Sigma® (S5631), selected via sedimentation according to Stokes' law, subjected to acid hydrolysis, and baked overnight (200 °C for 16 h) [14]. Antibodies against HECTD1 (sc-134976, rabbit), ZC3H12A (sc-136750, goat), GAPDH (sc-25778, rabbit) and ARG1 (sc-20150, rabbit) were obtained from Santa Cruz Biotechnology®, Inc. Antibodies against SOCS3 (2923S, rabbit) and NOS2 (ab 3523, rabbit) were purchased from CST and Abcam, Inc., respectively.

### Microarray and quantitative analyses

Agilent Feature Extraction software (version 11.0.1.1) was used to analyze the acquired array images. Quantile normalization and subsequent data processing were performed with the R software package. Additional details are provided in Supplementary Material.

### Cell culture

RAW264.7 and L929 (ScienCell) cells were cultured in DMEM supplemented with 10% fetal bovine serum (FBS), 100 U/mL penicillin, 100 μg/mL streptomycin and 2 mM L-GlutaMAX (obtained from Gibco®) at 37 °C in a humidified 5% $CO_2$ atmosphere.

### Western blotting

Western blotting assays were performed to determine cellular protein levels as previously described [14]. Briefly, after the treated cells were washed three times with cold phosphate-buffered saline (PBS), the cells were harvested using a mammalian cell lysis kit (MCL1-1KT, Sigma-Aldrich). Equal amounts of the proteins were then subjected to SDS-PAGE under reducing conditions, and the separated proteins were then transferred to PVDF membranes. The membranes were then blocked with 5% non-fat dry milk in Tris-buffered saline with Tween-20 (TBST) at room temperature for 1 h. The membranes were subsequently probed with the indicated antibodies overnight at 4 °C. After three additional washes, the membranes were incubated with an alkaline phosphatase-conjugated goat anti-mouse/rabbit or rabbit anti-goat IgG secondary antibody (1:5000 dilution). A chemiluminescence detection system was used to detect the resultant signals. The intensity of the protein bands was quantified via densitometry using ImageJ software (NIH). Each western blot was repeated at least five times.

### Quantitative reverse transcription-polymerase chain reaction (qRT-PCR)

RNAs were detected using qRT-PCR, The primers used in these assays are provided in Table S1. Additional details are provided in Supplementary Material.

### Immunoprecipitation

Immunoprecipitation assays were performed to detect the interactions between proteins as previously described [14]. Briefly, equal amounts of the proteins were incubated with an anti-ZC3H12A antibody overnight at 4 °C and then with 20 μL of protein A/G

PLUS-Agarose (sc-2003, Santa Cruz Biotechnology®, Inc.) for 90 min at 4 °C. The mixture was then centrifuged (13500 × g, 1 min, 4 °C), and the cell pellets were rinsed three times with RIPA lysis buffer. The cell pellets were subsequently boiled in western blot loading buffer for 5 min. After centrifugation (13500 × g, 1 min), the supernatants were subjected to western blotting for the detection of HECTD1.

### Cell migration assays

Cell migration assays were employed to examine fibroblast motility as previously described [14]. The cell gap was quantified using ImageJ software.

### 3-(4,5-Dimethylthiazol-2-yl)-2,5-diphenyltetrazolium bromide (MTT) assays

Cell viability was measured using MTT assays as previously described [14, 15].

### Human bronchoalveolar lavage fluid (BALF)

Human BALF was obtained from Nanjing Chest Hospital. Primary alveolar macrophages derived from human BALF were used in accordance with the approved guidelines from the Research and Development Committee of Nanjing Chest Hospital according to a previously described protocol [14]. Briefly, after filtering BALF through multilayer gauze, the BALF was centrifuged in a 50 mL centrifuge tube at 4 °C and 300 × g for 10 min. After the supernatant was discarded, the cells were resuspended in serum-free medium, counted with a hemocytometer and seeded in a 24-well plate at 5 × $10^5$ cells/well. After incubation of the cells for 2 h under 5% $CO_2$ at 37 °C, the serum-free medium was removed from the plate, and each well was washed twice with cold PBS to remove non-adherent cells and cell debris. The obtained cells, 95% of which were macrophages, were cultured in complete medium and employed for further experiments.

### Target DNA deletion/upregulation using clustered regularly interspaced short palindromic repeats (CRISPR)/CRISPR-associated protein 9 (Cas9) technology

Macrophages were transiently transfected with the CRISPR/Cas9 plasmids according to the manufacturer's recommended protocol (Santa Cruz®) to delete/upregulate HECTD1 and examine the downstream effects. The transfection efficiency was determined via western blotting. In brief, RAW246.7 cells were seeded at 2× $10^5$ cells per well in a 6-well plate, in 3 mL of antibiotic-free standard growth medium and grown to 40-80% confluency. Then, 300 µL of the Plasmid DNA/UltraCruz® Transfection Reagent Complex, consisting of 2 µg of plasmid DNA and 10 µL of the UltraCruz® Transfection Reagent in Plasmid Transfection Medium, was added dropwise to each well. Thereafter, gentle mixing was performed by swirling the plate, and the cells were incubated for 24-72 h under normal conditions to culture the cells prior to subsequent experiments.

### Lentiviral transfection

Cells were transfected with a lentivirus (HANBIO Inc., Shanghai, China) using a previously described method [15, 16].

### Immunofluorescence staining

Immunofluorescence staining was performed as previously described [15, 17].

### Statistics

The data are presented as the mean ± standard error of the mean (SEM). Unpaired numerical data were compared using an unpaired t-test (two groups) or analysis of variance (ANOVA; more than two groups). A P-value of $P<0.05$ was regarded as statistically significant.

## Results

### Differential expression of circRNAs in the lungs of mice exposed to $SiO_2$.

According to recent reports, circRNAs are involved in various diseases [6-10]. However, researchers have not determined whether circRNAs are also involved in the development of silicosis. In the present study, we performed a circRNA microarray analysis of an established mouse model of $SiO_2$-induced silicosis [18]. As shown in Figure 1A, circRNAs were expressed in the lungs of the normal saline (NS)- and $SiO_2$-treated mice, as revealed via hierarchical clustering. We identified 120 circRNAs that were differentially expressed in the $SiO_2$ group compared with the NS group. Seventy-three of these circRNAs were upregulated, and 47 were downregulated in the mouse model of silicosis. mmu_circ_0000375 (mm9_circ_002888/circHECTD1) was of particular interest because its host gene, HECTD1 (a candidate E3 ubiquitin ligase), might be involved in $SiO_2$-induced inflammation and fibrosis via ubiquitination. Based on previous data from our laboratory, ZC3H12A/MCPIP1 might mediate macrophage activation and fibroblast proliferation/migration via ubiquitination [14, 19, 20], but the detailed mechanism is unknown. As shown in the volcano and scatter plots presented in Figure 1B-C, circHECTD1 expression varied in the lungs of mice in the NS group and $SiO_2$ group, whereas Figure 1D shows the ID number and alias of mmu_circHECTD1 from the circBase database.

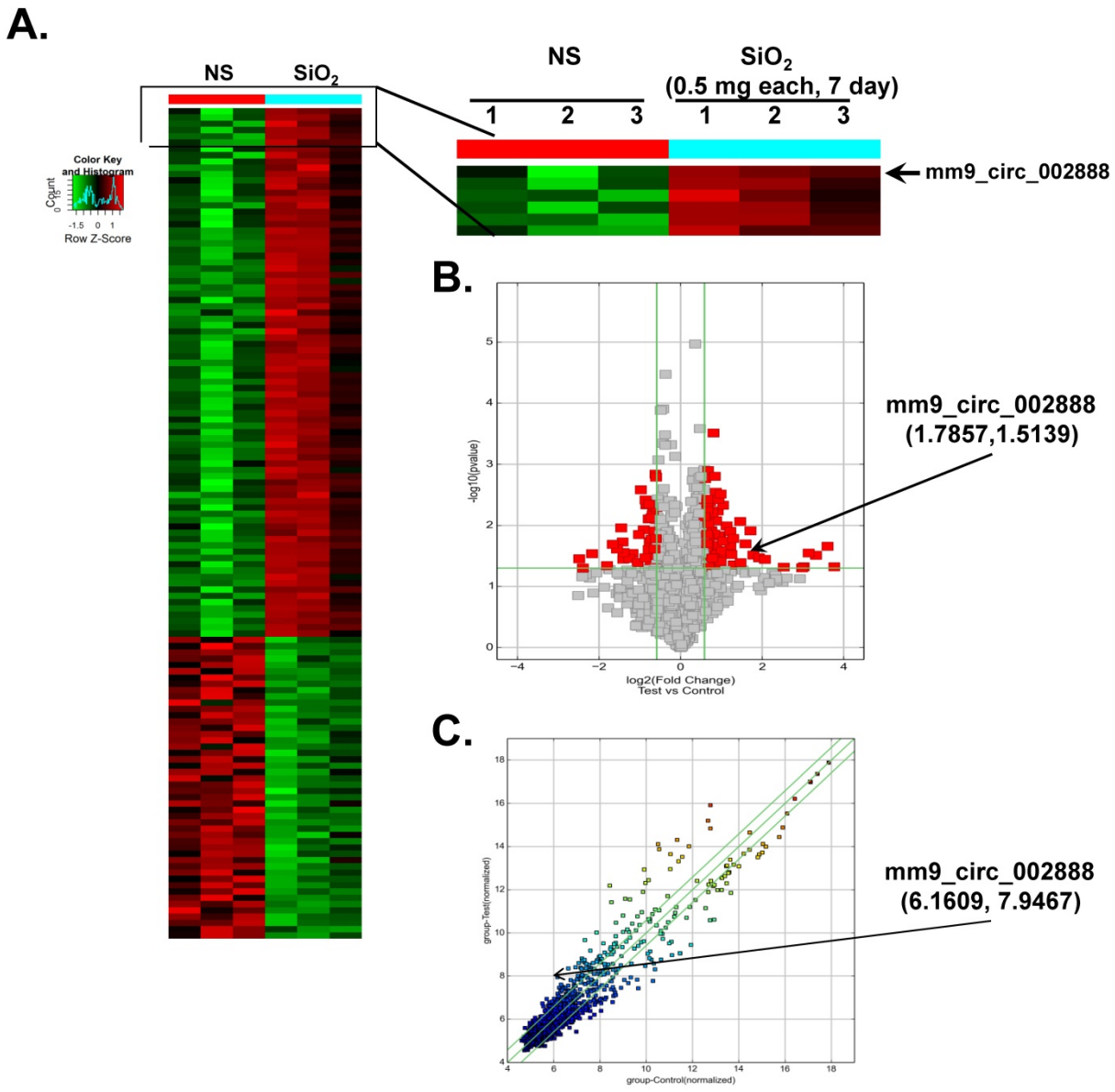


D.


**Figure 1. Differential expression of circRNAs in mouse lung tissues. (A)** Hierarchical clustering analysis of circRNAs that are differentially expressed in lung tissues from NS- and $SiO_2$-treated mice; each group contained three individuals (greater than a two-fold difference in expression; $P<0.05$). The expression levels are presented in different colors indicating expression levels above and below the median expression level across all samples. **(B)** Volcano plots were constructed using fold change values and *P*-values. The vertical lines correspond to 2.0-fold up- and downregulation between the NS- and $SiO_2$-treated groups, and the horizontal line represents the *P*-value. The red point in the plot represents the differentially expressed circRNAs showing statistical significance. **(C)** The scatter plot is used to visually assess the variations in circRNA expression between NS- and $SiO_2$-treated samples. The values corresponding to the X- and Y-axes in the scatter plot are the normalized signals of the samples ($Log_2$ scaled). The green lines indicate fold changes. The circRNAs above the top green line and below the bottom green line show a greater than 2.0-fold change between the NS- and $SiO_2$-treated groups. **(D)** ID number and alias of mmu_circ_0000375 from the circBase database.

### Expression of circHECTD1 in macrophages after exposure to $SiO_2$

Based on accumulating evidence, alveolar macrophages (AMOs) are the effector cells of silicosis [3, 5, 20]. AMOs are the most important immune barrier against invading pathogens and environmental contaminants in pulmonary innate immunity [14, 21]. Thus, the effect of $SiO_2$ on circHECTD1 expression was measured in mouse RAW264.7 macrophages. We experimentally determined the levels of circHECTD1 in RAW264.7 cells via qRT-PCR using divergent primers. As shown in Figure 2A, the divergent primers amplified circHECTD1 from cDNA, but not genomic DNA (gDNA). In contrast to the observations made in lung tissue, circHECTD1 expression decreased after 24 h of $SiO_2$ exposure in RAW264.7 cells (Figure 2B). These results were confirmed in a fluorescence *in situ* hybridization (FISH) assay, in which circHECTD1 was mainly detected in the cytoplasm of RAW264.7 cells (Figure 2C-D, Figure S1). To validate this *in vitro* finding, the circHECTD1 levels in macrophages isolated from $SiO_2$-treated mouse BALF were detected, and the results revealed that circHECTD1 was significantly decreased after 7 and 28 days compared with the levels in NS-treated mice (Figure 2E).

### circHECTD1 mediates macrophage activation in response to $SiO_2$ exposure

A circHECTD1 lentivirus was transfected into RAW264.7 cells to assess whether the observed changes in circHECTD1 expression were associated with the activation and apoptosis of the $SiO_2$-treated macrophages. As shown in Figure 3A, circHECTD1 was significantly upregulated in RAW264.7 cells transfected with the circHECTD1 lentivirus. The functional relevance of $SiO_2$-induced circHECTD1 downregulation was evaluated by measuring cell viability. As shown in Figure 3B, transfection of circHECTD1 in RAW264.7 cells restored the decrease in cell viability induced by the 48 h of exposure to $SiO_2$. Macrophage activation plays a significant role in the pathogenesis of pulmonary fibrosis [22]. The levels of various phenotypic markers of macrophages, such as NOS2 (M1), ARG1 (M2a) and SOCS3 (M2c), were measured in $SiO_2$-treated RAW264.7 cells to obtain a better understanding of the mechanism through which circHECTD1 activates macrophages. These markers were selected based on previous findings from our laboratory and are commonly accepted phenotypic markers of M1 and M2 macrophages [23, 24]. As shown in Figure 3C-D, $SiO_2$ induced a significant increase in the expression of NOS2, ARG2 and SOCS3. The expression of M2 markers peaked at 6 h, whereas the expression of M1 markers showed a later increase, at 24 h, and remained elevated until 48 h, indicating that the macrophages had undergone a phenotypic transformation. Transfection with the circHECTD1 lentivirus attenuated the phenotypic transformation of the macrophages treated with $SiO_2$ (Figure 3E-F). Moreover, circHECTD1 lentivirus transfection abrogated the increase in $SiO_2$-induced RAW264.7 cell migration, confirming the role of circHECTD1 in $SiO_2$-induced macrophage activation (Figure 3G).

### ZC3H12A is involved in circHECTD1-mediated macrophage activation in response to $SiO_2$

Our laboratory previously showed that ZC3H12A/MCPIP1 could mediate macrophage activation and fibroblast proliferation/migration [5, 14, 19, 20, 25]. As a transcription factor, ZC3H12A can shuttle between different cellular compartments to affect cell processes. In addition, ZC3H12A harbors a ribonuclease that can regulate its own mRNA level via a negative feedback loop [26]. circRNAs can interact with transcription factors to influence their translocation, which subsequently induces a series of cellular processes [8]. However, it is unclear whether circHECTD1 can mediate ZC3H12A to affect macrophage activation. As shown in Figure 4A-G, the ZC3H12A plasmid attenuated the increases in both M1 and M2 markers induced by $SiO_2$, whereas ZC3H12A siRNA aggravated the increases in both M1 and M2 markers induced by $SiO_2$. Moreover, we employed an RNA-binding protein immunoprecipitation (RIP) assay to determine whether there was a correlation between circHECTD1 and ZC3H12A. As shown in Figure 4H, ZC3H12A interacted with circHECTD1 but not HECTD1 mRNA.

### $SiO_2$ induces HECTD1 expression in RAW264.7 cells

Having determined the involvement of circHECTD1 in macrophage activation, we next sought to identify the role of HECTD1 in this process. Based on recent studies, circRNAs act as sponges to interact with and influence the expression of miRNAs [27] or compete with the pre-mRNA splicing machinery to inhibit host gene expression [13]. Thus, we first tested whether the levels of HECTD1 protein were altered in the $SiO_2$-treated RAW264.7 cells. As shown in Figure 5A-B, the levels of HECTD1 protein presented a rapid and sustained increase after $SiO_2$ treatment, and this finding was confirmed by immunostaining (Figure 5C). Moreover, the level of HECTD1 mRNA showed a rapid and transient increase and peaked at 3 h after $SiO_2$ exposure (Figure

5D). To validate our *in vitro* findings for HECTD1, a mouse silicosis model was employed, and a Sirius Red staining assay showed $SiO_2$-induced collagen deposition and incomplete pulmonary alveoli in lung tissues, indicating successful establishment of the silicosis mouse model (Figure 5E). Immunohistochemistry analysis revealed accumulation of macrophages in the lungs, as indicated by an increase in F4/80, a specific macrophage marker, suggesting the occurrence of an inflammatory cascade. Additionally, HECTD1 expression was upregulated in mouse lungs after SiO2 exposure, and the colocalization of HECTD1 with the macrophage marker F4/80 also increased (Figure 5F), confirming previous *in vitro* findings for HECTD1 in RAW264.7 cells.

## circHECTD1 mediates HECTD1 to regulate RAW264.7 activation in response to $SiO_2$ exposure

We subsequently determined whether HECTD1 was involved in circHECTD1-mediated macrophage activation. As expected, the transfection of RAW264.7 cells with the circHECTD1 lentivirus did not affect the HECTD1 mRNA levels (Figure 6A); however, HECTD1 protein expression was inhibited (Figure 6B-C), highlighting the link between circHECTD1 and HECTD1. To further understand the role of HECTD1 in $SiO_2$-induced macrophage activation, the CRISPR/Cas9 system was applied. As shown in Figure 6D-E, transfection with the HECTD1 CRISPR activation plasmid (ACT) and transfection with the CRISPR double nickase plasmid (NIC) upregulated and downregulated the expression of HECTD1 in RAW264.7 cells, respectively. In addition, ACT increased the expression of ARG1 and SOCS3 but not NOS2, whereas NIC increased NOS2 expression and decreased ARG1 and SOCS3 expression in these cells (Figure 6F-G). Furthermore, ACT aggravated $SiO_2$-induced ARG1 and SOCS3 expression after 6 h (Figure 6H-I) and $SiO_2$-induced NOS2 expression after 24 h (Figure 6J-K), and these $SiO_2$-induced effects were abolished by NIC treatment (Figure 6J-K). Based on these results, HECTD1 is suggested to be involved in the circHECTD1-mediated phenotypic changes induced by $SiO_2$. ACT treatment also decreased the viability of the RAW264.7 cells, whereas NIC treatment restored their viability (Figure 6L).

## HECTD1 mediates macrophage activation via ZC3H12A ubiquitination in response to $SiO_2$

HECTD1 is involved in ubiquitination because it encodes a novel protein homologous to the E6-AP C-terminal (HECT) domain-containing E3 ubiquitin (Ub) ligase [28]. Because both HECTD1 and ZC3H12A are involved in the ubiquitination process, it is reasonable to assume that they interact after $SiO_2$ exposure. Hence, ZC3H12A expression induced by $SiO_2$ was detected. As shown in Figure S2A-B, ZC3H12A expression increased in a time-dependent manner following exposure to $SiO_2$. In addition, an immunoprecipitation assay (Figure 7A) revealed an interaction between HECTD1 and ZC3H12A. The activity of ZC3H12A, a novel deubiquitinating enzyme (DUB), was abolished by mutation of its CCCH Zn finger domain (ΔZF) [29]. As shown in Figure 7B, mutation of the CCCH Zn finger domain of ZC3H12A attenuated the interaction between ZC3H12A and HECTD1. To explore the ubiquitination function of HECTD1 in macrophage activation, the effects of MG-132, a proteasome inhibitor, on ZC3H12A were detected. As shown in Figure S2C-E, the viability of RAW264.7 cells was decreased in a dose-dependent manner. Furthermore, ZC3H12A expression was elevated after physiological exposure to MG-132 but not after $SiO_2$ treatment. Subsequently, the effects of HECTD1 on K48-ubiquitin expression were detected. As shown in Figure 7C, overexpression of HECTD1 enhanced K48-ubiquitin expression. HECTD1 knockdown attenuated K48-ubiquitin expression, whereas the effect on ZC3H12A expression was opposite that of K48-ubiquitin (Figure 7D-E). Moreover, transfection of the circHECTD1 lentivirus decreased K48-ubiquitin expression (Figure S2F). Taken together, these results indicate that HECTD1 might induce ZC3H12A degradation via ubiquitination. Therefore, further immunoprecipitation experiments using either HECTD1-ACT or HECTD1-NIC were performed. As shown in Figure 7F, HECTD1-ACT enhanced the interaction between ZC3H12A and K48-ubiquitin, whereas HECTD-NIC attenuated this interaction, indicating that HECTD1-mediated ZC3H12A expression occurred via ubiquitination. To further understand the events downstream of HECTD1-mediated ZC3H12A ubiquitination, the inflammatory cytokines IL-1β, IL-6, and IL-12p40 and the signaling molecule NF-κB (p65) were investigated. As shown in Figure S3A-B, the HECTD1-mediated changes in IL-1β and IL-6 mRNA, but not IL-12p40 mRNA, were recovered via pretreatment with MG-132. Additionally, the phosphorylation of NF-κB induced by HECTD1-ACT was attenuated by pretreatment with MG-132 (Figure S3C-D), whereas HECTD1-NIC inhibited the phosphorylation of NF-κB with or without MG-132 (Figure S3E-F).

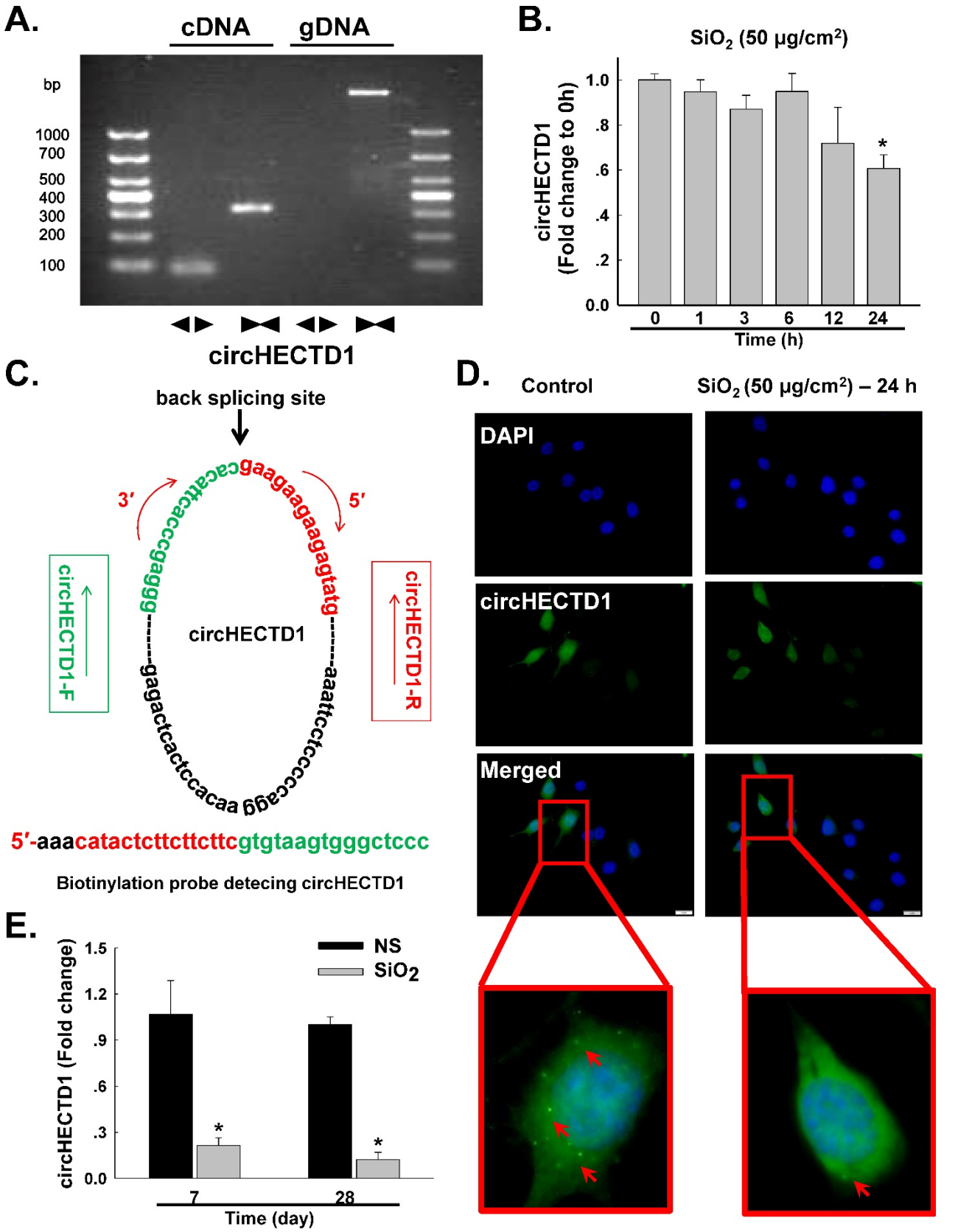


**Figure 2. circHECTD1 expression in macrophages exposed to $SiO_2$. (A)** Divergent primers amplified circRNAs from cDNAs but not genomic DNA (gDNA). **(B)** As shown in the qRT-PCR analysis, circHECTD1 was expressed in RAW264.7 cells exposed to $SiO_2$ (n=5). *$P$<0.05 vs. circHECTD1 expression at 0 h. **(C)** Structures and probe sequence of circHECTD1. **(D)** Fluorescence *in situ* hybridization assay showing circHECTD1 expression in RAW264.7 cells exposed to $SiO_2$. circHECTD1 was labeled with fluorescein isothiocyanate. Scale bar=5 μm. **(E)** circHECTD1 isolated from macrophages from mouse bronchoalveolar lavage fluid (BALF) was detected after saline or $SiO_2$ treatment on day 7 or 28. *$P$<0.05 vs. circHECTD1 expression in saline-treated groups.

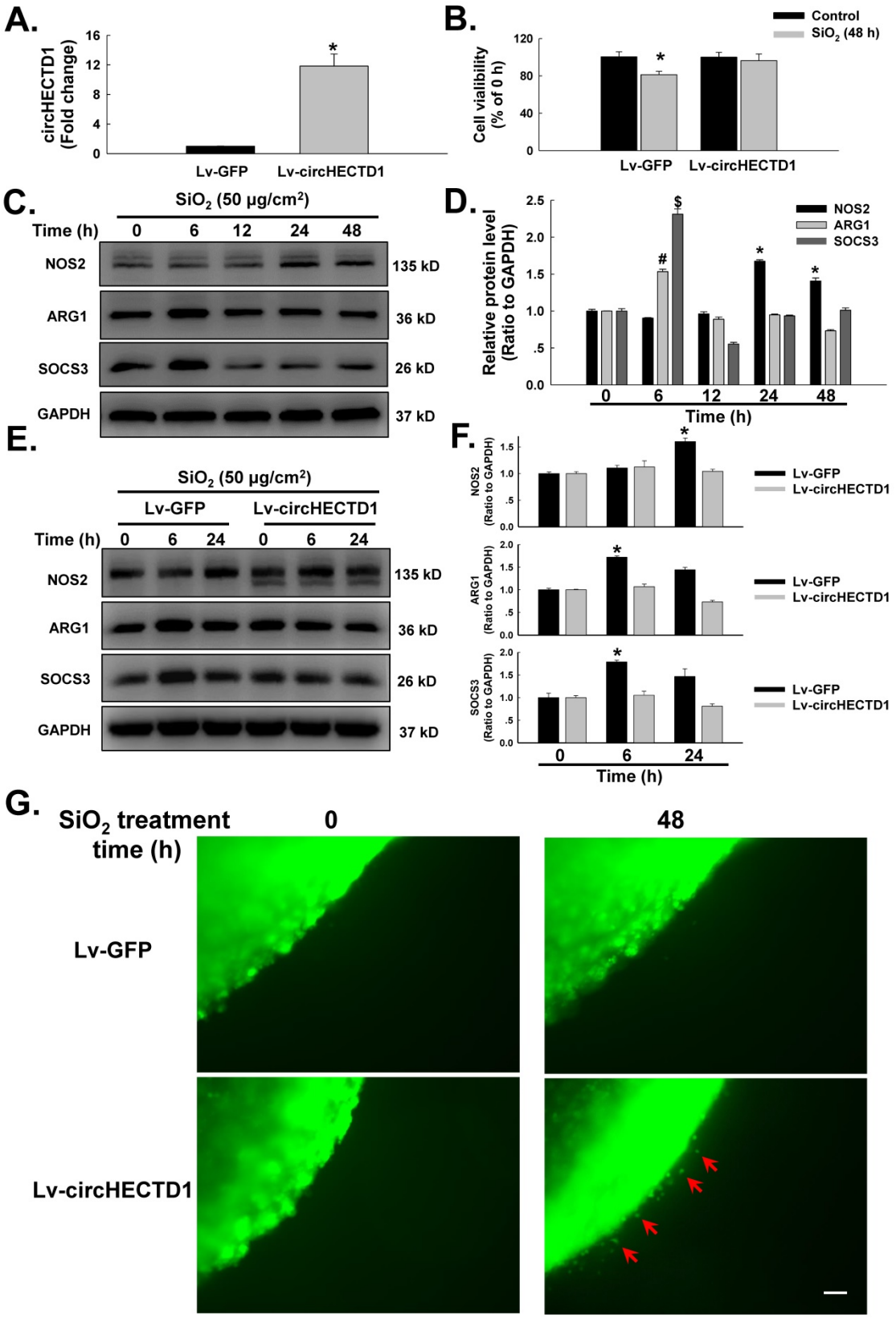


**Figure 3. circHECTD1 mediates macrophage activation in response to $SiO_2$. (A)** As shown in the qRT-PCR analysis, transfection of the circHECTD1 lentivirus upregulated circHECTD1 expression in RAW264.7 cells (n=5). **(B)** According to the results of the MTT assay, transfection of the circHECTD1 lentivirus attenuated the $SiO_2$-induced decrease in the viability of RAW264.7 cells (n=5); **P*<0.05 vs. the control group. **(C)** Representative western blot showing the effects of $SiO_2$ (50 μg/cm$^2$) on the expression of the M1 marker NOS2, the M2a marker ARG1 and the M2c marker SOCS3 in RAW264.7 cells. **(D)** Densitometric analyses of five separate experiments suggested that $SiO_2$ induced NOS2, ARG1 and SOCS3 expression in a time-dependent manner. **P*<0.05 vs. NOS2 expression at 0 h; #*P*<0.05 vs. ARG1 expression at 0 h; $*P*<0.05 vs. SOCS3 expression at 0 h. **(E)** Representative western blot showing the effects of circHECTD1 lentivirus transfection on $SiO_2$-induced NOS2, ARG1 and SOCS3 expression in RAW264.7 cells. **(F)** Densitometric analyses of five separate experiments suggested that $SiO_2$-induced NOS2, ARG1 and SOCS3 expression was attenuated by circHECTD1 lentivirus transfection. **P*<0.05 vs. the expression of the corresponding protein in the control group. **(G)** Representative images of the nested collagen matrix showing that the activation of RAW264.7 cells was inhibited by $SiO_2$, an effect that was reversed by circHECTD1 lentivirus transfection. Scale bar=80 μm.

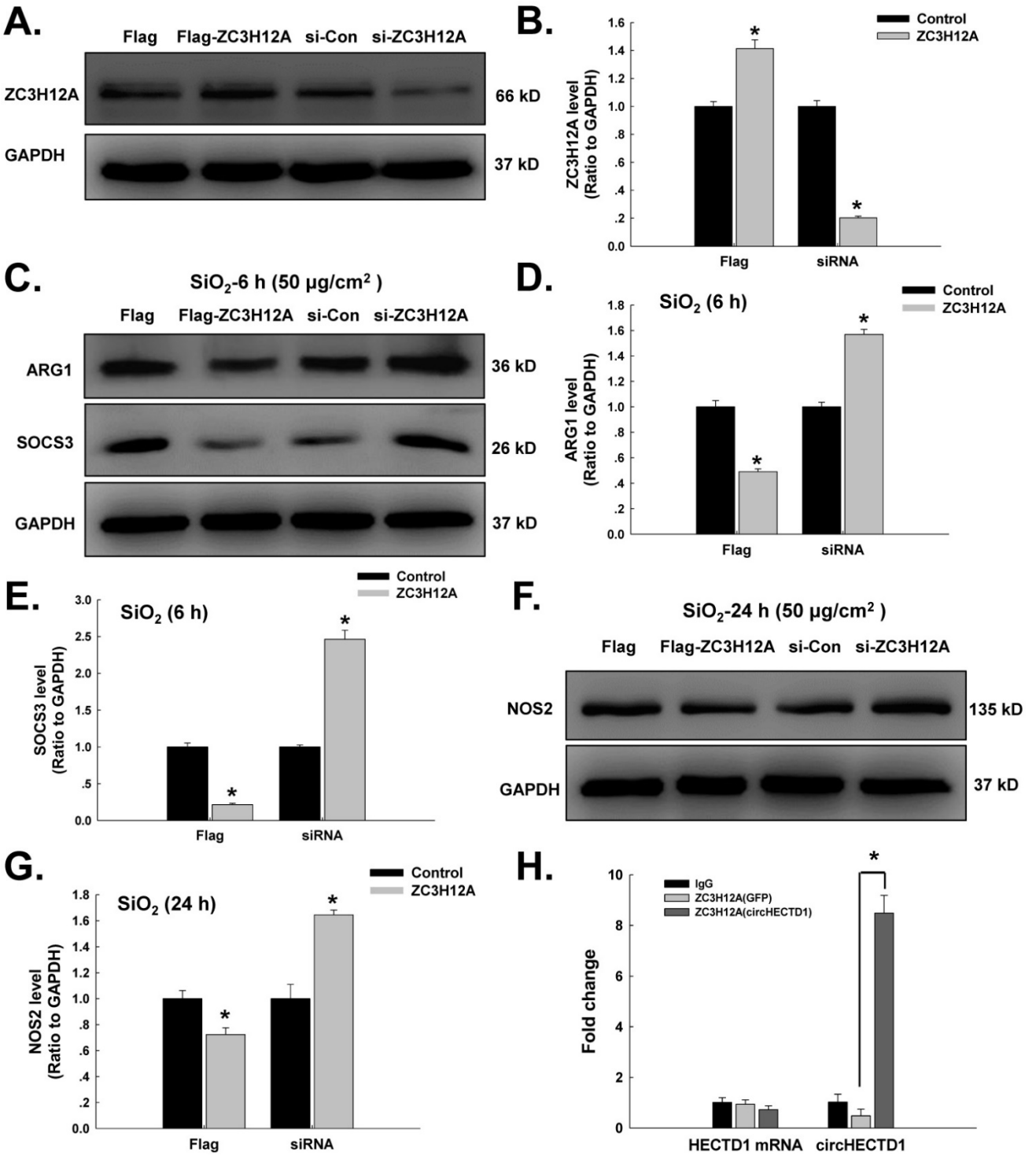


**Figure 4. ZC3H12A is involved in circHECTD1-mediated macrophage activation in response to $SiO_2$. (A)** Representative western blot showing that ZC3H12A plasmid or siRNA transfection upregulated or downregulated ZC3H12A expression, respectively, in RAW264.7 cells. **(B)** Densitometric analyses of five separate experiments suggested that ZC3H12A plasmid or siRNA transfection upregulated and downregulated ZC3H12A expression, respectively, in RAW264.7 cells (n=5); **P*<0.05 vs. the control group. **(C)** Representative western blot showing the effects of ZC3H12A plasmid and siRNA transfection on $SiO_2$-induced ARG1 and SOCS3 expression in RAW264.7 cells. Densitometric analyses of five separate experiments suggested that $SiO_2$-induced ARG1 **(D)** and SOCS3 **(E)** expression was attenuated by ZC3H12A plasmid transfection but enhanced by ZC3H12A siRNA transfection. **P*<0.05 vs. the corresponding control group. **(F)** Representative western blot showing the effects of ZC3H12A plasmid and siRNA transfection on $SiO_2$-induced NOS2 expression in RAW264.7 cells. **(G)** Densitometric analyses of five separate experiments suggested that $SiO_2$-induced NOS2 expression was attenuated by ZC3H12A plasmid transfection but enhanced by ZC3H12A siRNA transfection. **P*<0.05 vs. the corresponding control group. **(H)** Cell lysates prepared from cells were subjected to immunoprecipitation with antibodies against IgG and ZC3H12A and to real-time polymerase chain reaction. The antibody against ZC3H12A pulled down circHECTD1 but not HECTD1 mRNA.

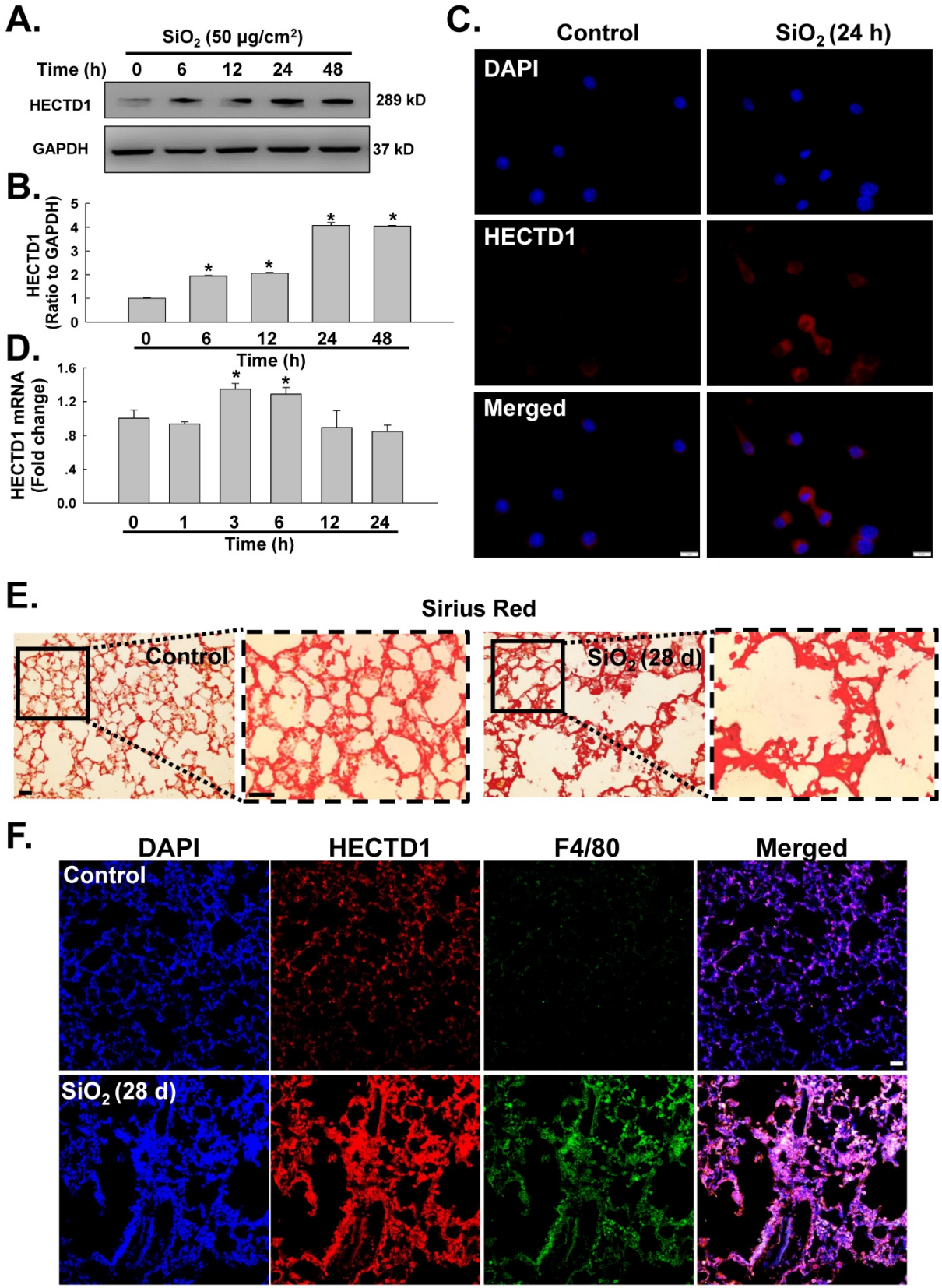


**Figure 5. $SiO_2$ induces HECTD1 expression in RAW264.7 cells. (A)** Representative western blot showing the effects of $SiO_2$ (50 μg/cm²) on HECTD1 expression in RAW264.7 cells. **(B)** Densitometric analyses of five separate experiments suggested that $SiO_2$ induced HECTD1 expression in a time-dependent manner. *$P$<0.05 vs. 0 h. **(C)** Representative images of immunocytochemical staining showing that $SiO_2$ (50 μg/cm²) increased HECTD1 expression in RAW264.7 cells 24 h after $SiO_2$ treatment. Scale bar=5 μm. **(D)** As shown in the qRT-PCR analysis, the expression of HECTD1 mRNA increased after RAW264.7 cells were exposed to $SiO_2$ (n=5); *$P$<0.05 vs. 0 h. **(E)** Sirius Red staining showing that $SiO_2$ induced more collagen deposition and incomplete pulmonary alveoli in the lung tissues, indicating that the silicosis mouse model was successfully induced. The images are representative of several individuals from each group (n=5). Scale bar=20 μm. **(F)** Immunohistochemistry detection of the macrophage marker F4/80 and HECTD1 in mouse lung tissues. Both F4/80 and HECTD1 expression presented an increasing tendency in $SiO_2$-treated mouse lung tissues, and lung tissues with $SiO_2$-induced silicosis exhibited more colocalization. In addition, the construction of pulmonary alveoli displayed serious damage in silicosis mouse lung tissues. The images are representative of several individuals from each group (n=5). Scale bar=20 μm.

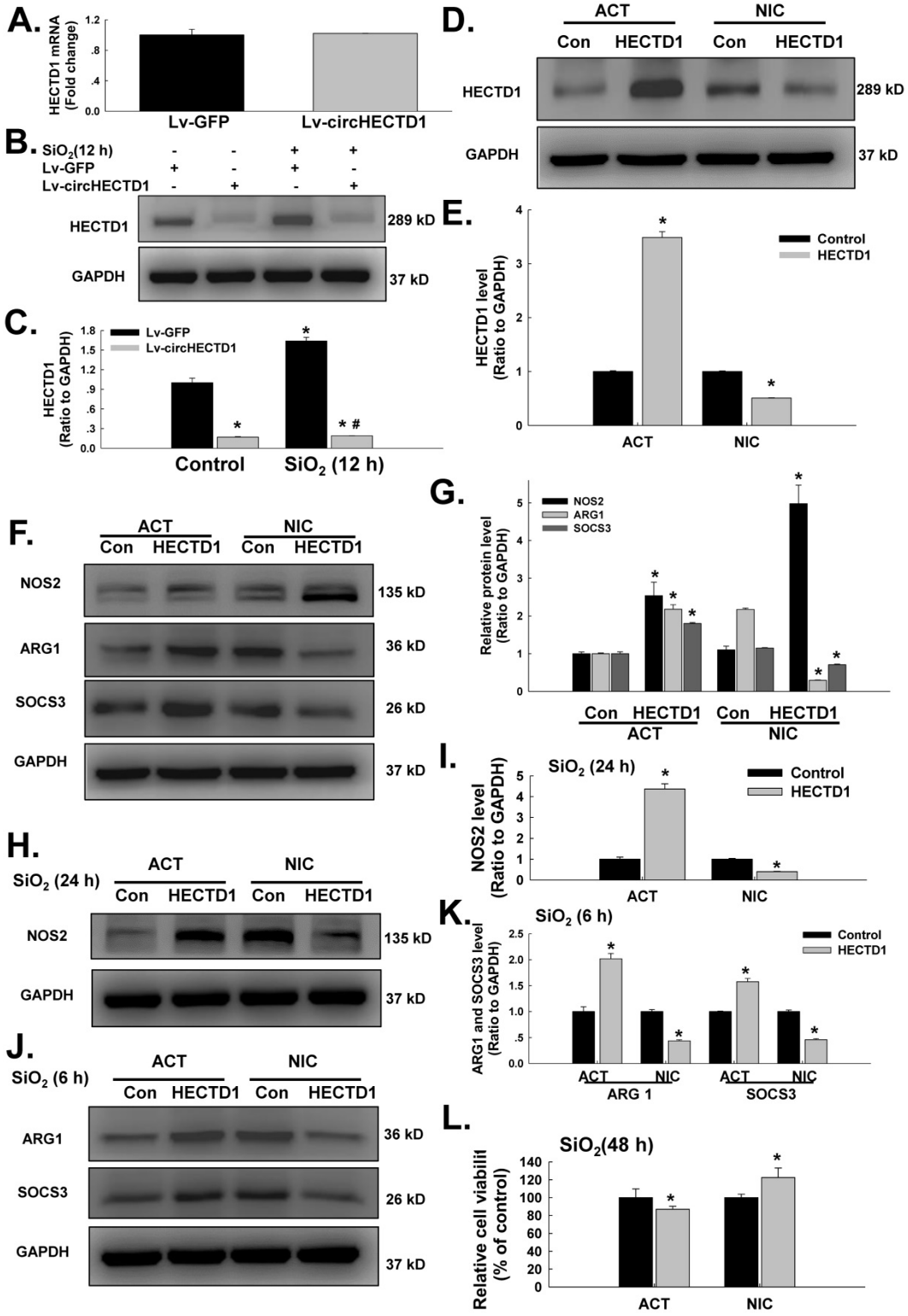


**Figure 6. circHECTD1-mediated HECTD1 expression regulates RAW264.7 cell activation in response to $SiO_2$ exposure. (A)** As shown in the qRT-PCR analysis, circHECTD1 lentivirus transfection did not affect the expression of HECTD1 mRNA in RAW264.7 cells (n=5); *$P$<0.05 vs. 0 h. **(B)** Representative western blot showing the effects of circHECTD1 lentivirus transfection on $SiO_2$-induced HECTD1 expression in RAW264.7 cells. **(C)** Densitometric analyses of five separate experiments suggested that circHECTD1 lentivirus transfection attenuated the $SiO_2$-induced increase in HECTD1 expression in RAW264.7 cells (n=5); *$P$<0.05 vs. the control group; #$P$<0.05 vs. the $SiO_2$ group. **(D)** Representative western blot showing that transfection with ACT or NIC upregulated and downregulated HECTD1 expression, respectively, in RAW264.7 cells. **(E)** Densitometric analyses of five separate experiments suggested that transfection with HECTD1 ACT and NIC upregulated and downregulated HECTD1 expression, respectively, in RAW264.7 cells (n=5); *$P$<0.05 vs. the control group. **(F)** Representative western blot showing the effects of ACT and NIC transfection on NOS2, ARG1 and SOC3 expression in RAW264.7 cells. **(G)** Densitometric analyses of five separate experiments suggested that HECTD1 ACT and NIC transfection affected NOS2, ARG1 and SOC3 expression in RAW264.7 cells (n=5); *$P$<0.05 vs. the corresponding control group. **(H)** Representative western blot showing the effects of HECTD1 ACT and NIC transfection on $SiO_2$-induced NOS2 expression in RAW264.7 cells. **(I)** Densitometric analyses of five separate experiments suggested that $SiO_2$-induced NOS2 expression was enhanced by HECTD1 ACT transfection but attenuated by HECTD1 NIC transfection. *$P$<0.05 vs. the corresponding control group. **(J)** Representative western blot showing the effects of HECTD1 ACT and NIC transfection on $SiO_2$-induced ARG1 and SOCS3 expression in RAW264.7 cells. **(K)** Densitometric analyses of five separate experiments suggested that $SiO_2$-induced ARG1 and SOCS3 expression was enhanced by HECTD1 ACT transfection but attenuated by HECTD1 NIC transfection. *$P$<0.05 vs. the corresponding control group. **(L)** MTT assay showing the effect of HECTD1 ACT and HECTD1 NIC transfection on the viability of RAW264.7 cells (n=5); *$P$<0.05 vs. the corresponding control group.

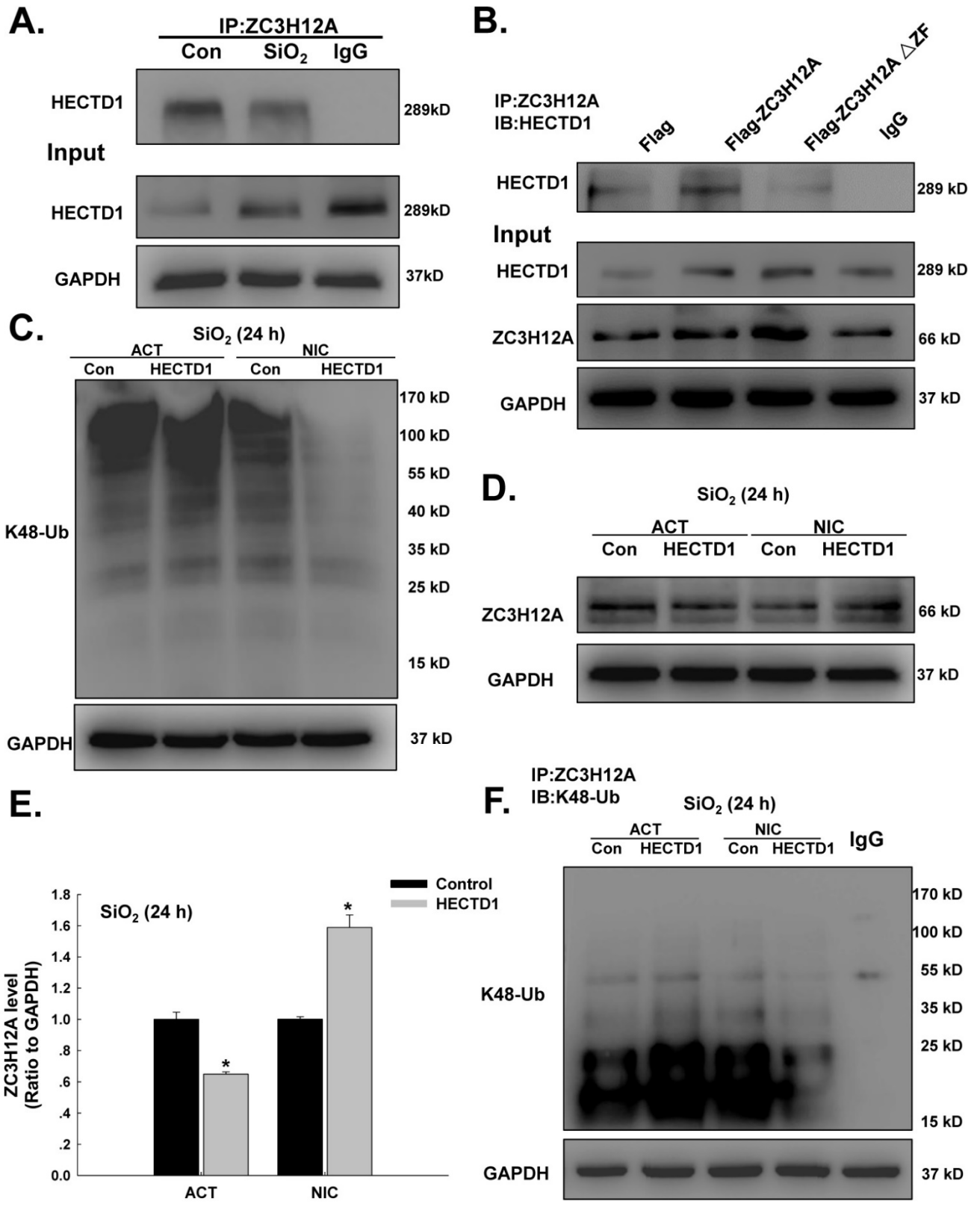


**Figure 7. HECTD1 mediates macrophage activation via ZC3H12A ubiquitination in response to $SiO_2$. (A) T**he interaction between ZC3H12A and HECTD1 in response to $SiO_2$ exposure examined by immunoprecipitation of ZC3H12A was performed in whole-cell lysates followed by immunoblotting for HECTD1. (B) RAW264.7 cells were transfected with Flag-ZC3H12A or a mutant version of the protein in which the CCCH Zn finger domain was truncated, as indicated. The interaction between HECTD1 and ZC3H12A was partially attenuated by the CCCH Zn finger domain mutation (△ZF) in ZC3H12A. **(C)** Effects of HECTD1 ACT and NIC transfection on $SiO_2$-induced K48-ubiqutin expression in RAW264.7 cells. K48-ubiqutin expression was enhanced by HECTD1 ACT transfection but attenuated by HECTD1 NIC transfection. **(D)** Representative western blot showing the effects of HECTD1 ACT and NIC transfection on $SiO_2$-induced ZC3H12A expression in RAW264.7 cells. **(E)** Densitometric analyses of five separate experiments suggested that $SiO_2$-induced ZC3H12A expression was attenuated by HECTD1 ACT transfection but enhanced by HECTD1 NIC transfection. *$P$<0.05 vs. the corresponding control group. **(F)** RAW264.7 cells were transfected with the HECTD1 ACT and NIC plasmids, and whole-cell lysates were then immunoprecipitated with the anti-ZC3H12A antibody and subsequently immunoblotted with the anti-K48-ubiquitin antibody to examine the interaction between ZC3H12A and K48-ubiquitin in response to $SiO_2$ exposure.

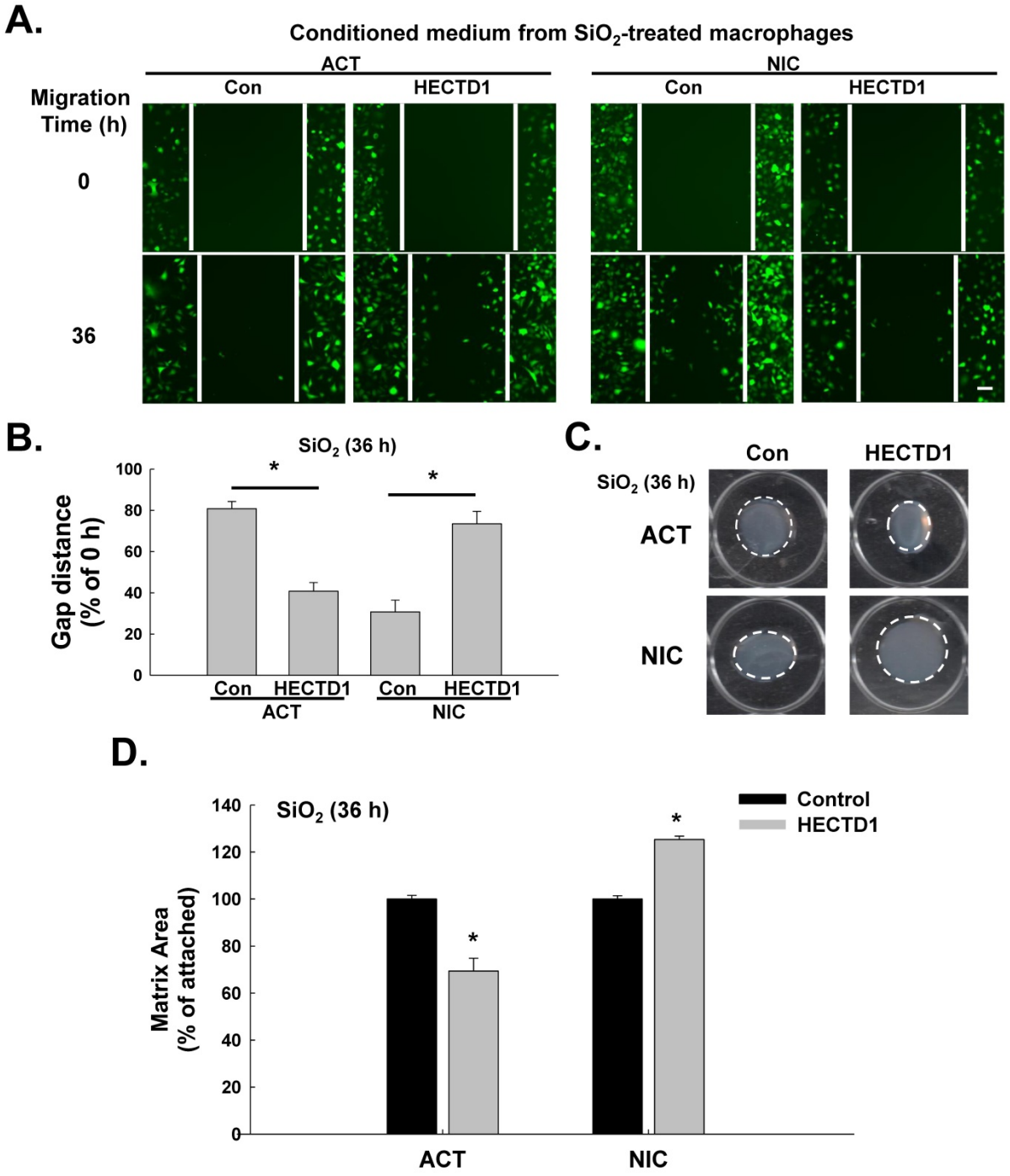


**Figure 8. $SiO_2$-induced upregulation of HECTD1 in macrophages is involved in fibroblast activation and migration. (A)** Representative images showing the effects of the conditioned media from RAW264.7 cells on the migration of GFP-labeled L929 cells. Scale bar=80 μm. **(B)** Quantification of scratch widths in six separate experiments. **P*<0.05 vs. the corresponding control group. **(C)** Representative images of collagen gel size showing the effects of the conditioned media from macrophages on gel contraction (indicating fibroblast activation). **(D)** Quantification of the matrix area in six separate experiments. **P*<0.05 vs. the corresponding control group.

## $SiO_2$-induced upregulation of HECTD1 in macrophages is involved in fibroblast activation and migration

Based on accumulating evidence, $SiO_2$-induced macrophage activation initiates pulmonary fibrosis, which is characterized by fibroblast activation and migration [30, 31]. Therefore, we subsequently explored whether HECTD1-induced macrophage activation is also involved in changes in fibroblast function. The supernatants from RAW264.7 cells exposed to $SiO_2$ in the presence or absence of ACT or NIC treatment (conditioned medium) were applied to fibroblasts, and fibroblast proliferation and migration were measured. As shown in Figure 8A-B, the

supernatants from the NIC-treated RAW264.7 cells significantly inhibited $SiO_2$-induced cell migration, whereas the supernatants from the ACT-treated RAW264.7 cells increased cell migration. In addition, the supernatants from normal physiological RAW264.7 cells grown in the presence or absence of ACT or NIC (conditioned medium) exerted the same effects on fibroblast migration (Figure S4A-B). The results of the matrix contraction assay, which is commonly employed to evaluate fibroblast activation, are shown in Figure 8C-D. The supernatants from the NIC-treated RAW264.7 cells caused significant inhibition of $SiO_2$-induced fibroblast activation, whereas the supernatants from the ACT-treated RAW264.7 cells caused increased fibroblast activation.

## HECTD1 expression is increased in macrophages from patients with silicosis

Previous results from our laboratory have suggested that macrophage activation and apoptosis marker expression are increased in macrophages from the BALF of patients with silicosis [14]. Hence, we next extended our cell culture experiments to an examination of patients with silicosis to validate our findings. As shown in Figure 9A-B, HECTD1 levels were significantly increased in macrophages from the BALF of patients with silicosis compared with those from healthy donors. Moreover, we observed colocalization between HECTD1 and the macrophage marker F4/80 in the lung tissues of patients with silicosis (Figure 9C). Based on these results, macrophages from patients with silicosis showed increased HECTD1 levels and underwent apoptosis and activation, thus promoting the development of silicosis.

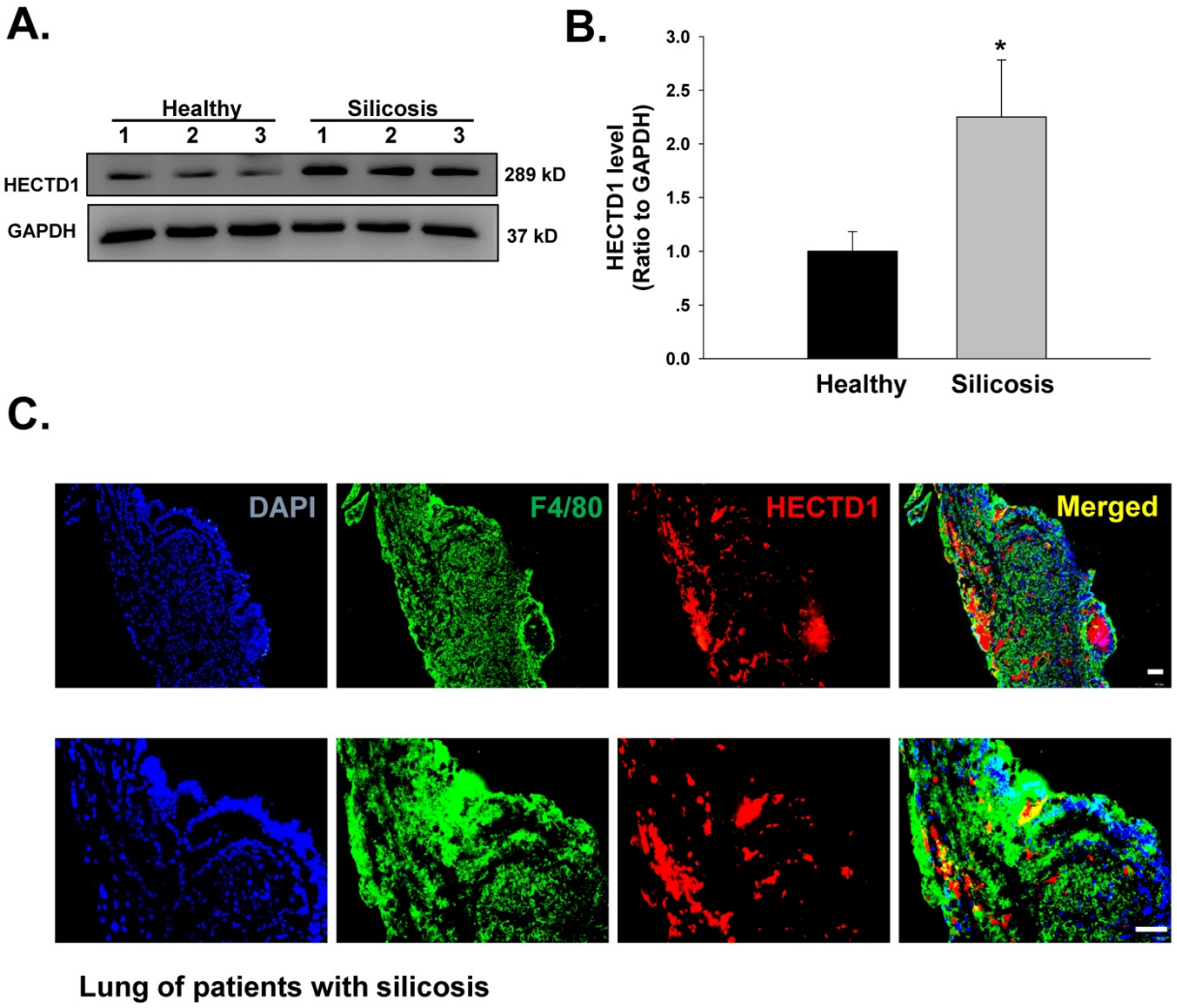


**Figure 9. HECTD1 expression is increased in macrophages from patients with silicosis. (A)** Representative western blot showing HECTD1 expression in macrophages from healthy donors and patients with silicosis. **(B)** Densitometric analyses of macrophage samples from five healthy donors and five patients with silicosis suggested that HECTD1 expression was elevated in macrophages from patients with silicosis. *$P$<0.05 vs. the corresponding healthy control group. **(C)** Immunohistochemistry of the macrophage marker F4/80 and HECTD1 in lung tissues from patients with silicosis. Colocalization between F4/80 and HECTD1 is shown. The images are representative of several individuals from each group (n=5). Scale bar=20 μm.

## Discussion

Alveolar macrophages respond to particles inhaled through the pulmonary bronchial airway via intricate interactions with other cells, such as fibroblasts and epithelial cells. These macrophages function as effector cells by secreting and releasing factors that attract and regulate other cells, resulting in continuous increases in mesenchymal components [5, 32]. Many efforts have been made to prevent macrophage activation and fibrosis in silicosis. However, no effective therapies or drugs are currently available to prevent or minimize the progression of $SiO_2$-induced inflammation [33].

Depending on environmental stimuli, macrophages differentiate into heterogeneous phenotypes, including the classically activated M1 phenotype and the alternatively activated M2 phenotype [34]. M1 macrophages are associated with inflammation because they secrete proinflammatory cytokines and produce large amounts of nitric oxide [35]. In contrast, M2 macrophages are associated with ARG1 upregulation, leading to enhanced biosynthesis of proline and polyamine, which play important roles in cell proliferation, tissue repair and collagen production [34]. In the present study, $SiO_2$ was found to induce a dramatic, late increase in the levels of NOS2 protein (M1 marker) and an early increase in the levels of SOCS3 and ARG1 proteins (M2 markers) in macrophages, suggesting that both activation signals and M1/M2 transformation are involved in silicosis pathology, which is consistent with the findings of previous studies [36].

circRNAs are widely expressed noncoding RNAs that are unusually stable, but the functions of circRNAs are poorly understood [13]. A recent study on circRNAs defined important roles for these RNAs in development, heart senescence, heart hypertrophy, heart failure and cell growth [8, 10, 37-39]. Here, we performed a circRNA microarray analysis of lung samples from $SiO_2$-treated mice and revealed the first expression profile of circRNAs in a mouse model of silicosis, which showed 73 upregulated and 47 downregulated circRNAs. Based on a bioinformatic analysis and a previous study from our laboratory, circHECTD1 attracted our attention because the host gene of circHECTD1, HECTD1, is an E3 ubiquitin ligase that regulates the cell migration machinery [40]. Interestedly, previous results from our laboratory showed that the deubiquitinase MCPIP1/ZC3H12A is also involved in $SiO_2$-induced macrophage activation, cell migration and the endothelial-to-mesenchymal transition (EndMT) [14, 15, 20, 25]. The current study primarily focused on the role of circHECTD1 in macrophage activation and showed that circHECTD1 prevented the $SiO_2$-induced changes in M1/M2 phenotypes and the decrease in cell viability, indicating a preventative effect of circHECTD1 on macrophage activation. Based on recent studies, circRNAs act as sponges that interact with miRNAs and influence the expression of target proteins [27] or compete with the pre-mRNA splicing machinery to inhibit host gene expression [13]. In the current study, the observed decrease of circHECTD1 expression in combination with the increased HECTD1 mRNA levels indicated the involvement of a pre-mRNA competition mechanism. Although further experiments are needed to clarify the detailed mechanism, the current results reveal the connection between circHECTD1 and HECTD1.

Notably, circHECTD1 expression in macrophages was downregulated in response to $SiO_2$ exposure, a finding that contrasts with circHECTD1 expression in the lungs of silicosis mice. One possible explanation for these results is that the initiation of inflammation induced by $SiO_2$ recruits monocytes to the lungs to differentiate into macrophages, ultimately causing an inflammatory cascade. As a result, although circHECTD1 decreases in macrophages after $SiO_2$ exposure, the accumulation of macrophages in the lungs will increase the level of circHECTD1 in the whole lung. In contrast, silicosis is characterized by progressive pulmonary fibrotic reactions involving different types of cells, such as macrophages, endothelial cells, epithelial cells and fibroblasts [3, 41-43]. Pulmonary fibroblasts are a type of dendritic cell found in the lung that acts as the main contributor to fibrosis in the late stage of silicosis. Although clinical evidence has indicated that the activation of alveolar macrophages by $SiO_2$ causes rapid and sustained inflammation as well as cytokine and chemokine production, which, in turn, induce fibrosis, recent studies have suggested that the direct effect of $SiO_2$ on dendritic cells (e.g., on their proliferation and migration) also plays an important role in the pathogenesis of fibrosis [31]. The question of whether over-proliferation associated with changes in circHECTD1 expression in fibroblasts contributes to the upregulation observed in the lungs of silicosis mice deserves further investigation. Moreover, the fibrosis generated via EndMT and EMT also underlies the accumulation of fibroblasts in silicosis [25]. The contradictory observations regarding circHECTD1 expression might be due to the differences in its expression patterns in different types of cells in the lungs; for example, circHECTD1 expression is upregulated in endothelial cells, which promotes EndMT (data not shown), suggesting that circHECTD1 plays multiple roles in silicosis.

HECTD1 encodes a novel protein homologous to the E6-AP C-terminal (HECT) domain-containing E3

ubiquitin (Ub) ligase, which regulates the selective ubiquitination of Hsp90 client proteins [28, 44]. HECTD1 is involved in cell migration via PIPKIγ90 [45]; in neural tube defects and abnormal cranial mesenchyme via Hsp90 [28]; and in the regulation of Wnt signaling via APC-Axin interactions [46]. Interestingly, HECTD1 regulates cell polarity by ubiquitinating key proteins [40]. Moreover, HECTD1 expression is upregulated in fibroblasts obtained from the primary sites, lymph nodes and bone marrow of patients with breast cancer [47], indicating that HECTD1 might be involved in two important $SiO_2$-induced steps: silicosis-macrophage polarization and fibroblast migration/proliferation [14, 20, 25]. In the current study, HECTD1 was found to promote macrophage polarization, as indicated by the upregulation of both M1 and M2 markers, which decreased cell viability. Furthermore, HECTD1 was found to be involved in the effects of macrophages on fibroblast migration, suggesting a key role of HECTD1 in silicosis.

ZC3H12A, also known as MCPIP1 or Regnase-1, is a novel RNA-binding protein (RBP) that plays a key role in post-transcriptional regulation and immune homeostasis [26, 48]. Post-transcriptional control can occur at each step of RNA metabolism. Recently, mRNA degradation and translation have received significant attention due to their role in the regulation of immune responses [49]. In monocytes, ZC3H12A downregulates IL-1β, IL-6, and IL-12p40 through degradation of their mRNAs [26, 48]. ZC3H12A can also target its own mRNA to promote its degradation. Moreover, the ZC3H12A protein can be degraded by the ubiquitin-proteasome system [50]. This study found that ZC3H12A could be sequestered in the cytoplasm by circHECTD1 to affect macrophage activation, possibly due to inhibited feedback regulation of inflammatory responses induced by ZC3H12A. After RAW264.7 cells were treated with MG-132, ZC3H12A was upregulated; however, treatment with MG-132 and $SiO_2$ downregulated the expression of ZC3H12A, which might be due to self-degradation via its own feedback regulation. In addition, ZC3H12A was degraded via the ubiquitin-proteasome system, which was induced by HECTD1. These results suggest that ZC3H12A is involved in circHECTD1/HECTD1-mediated macrophage activation.

Furthermore, our analyses of primary alveolar macrophages from patients suggested that HECTD1 expression was increased concomitantly with macrophage apoptosis and activation compared with primary alveolar macrophages from healthy donors, consistent with our *in vitro* results. Thus, both our *in vivo* and *in vitro* results confirmed the clinical significance of our findings and revealed that HECTD1 may serve as a potential marker of silicosis.

## Conclusion

Our study elucidated a link between $SiO_2$-induced macrophage activation and the circHECTD1/HECTD1 pathway, thereby providing insight into the potential use of HECTD1 to develop novel therapeutic strategies for treating silicosis (Figure 10).

## Abbreviations

$SiO_2$: silicon dioxide; MCPIP1: monocyte chemotactic protein-1-induced protein 1; HECTD1: HECT domain E3 ubiquitin protein ligase 1; circRNAs: circular RNAs; ceRNAs: competing endogenous RNAs; DMEM: Dulbecco's modified Eagle's medium; NS: normal saline; FBS: fetal bovine serum; siRNA: small interference RNA; MTT: 3-(4,5-dimethylthiazol-2-yl)-2,5-diphenyltetrazolium bromide; FISH: Fluorescence in situ hybridization; AMOs: alveolar macrophages; PFBs: pulmonary fibroblasts.

## Supplementary Material

Detail of microarray and quantitative analyses, fluorescent in situ hybridization (FISH), RNA-binding protein immunoprecipitation (RIP) and quantitative reverse transcription-polymerase chain reaction (qRT-PCR). Supplementary Figures S1–S4 and Table S1. http://www.thno.org/v08p0575s1.pdf

## Acknowledgments

This study is the result of work that was partially supported by the resources and facilities of the core laboratory at the Medical School of Southeast University.

### Sources of support

National Natural Science Foundation of China (Nos. 81773796, 81473263, 81400300 and 81600045).

Natural Science Foundation of Jiangsu Province, China (No. BK20141347).

Postgraduate Research & Practice Innovation Program of Jiangsu Province KYCX17_0165.

### Author contributions

Z.Z. performed the experiments, interpreted the data, prepared the figures, and wrote the manuscript. R.J., X.Y., H.G., S.F., Y.Z., Y.C. and J.W. performed the experiments and interpreted the data. H.Y. designed the experiments, interpreted the data, and wrote the manuscript. J.C. provided laboratory space and funding, designed the experiments, interpreted the data, wrote the manuscript, and directed the project.

All authors read, discussed, and approved the final manuscript.

### Ethics approval and consent to participate

All participants provided written informed consent prior to participating in the study. The primary alveolar macrophages derived from human BALF were employed in accordance with the approved guidelines from the Research and Development Committee of Nanjing Chest Hospital (2016-KL002-01), and all procedures were conducted in accordance with the Declaration of Helsinki.

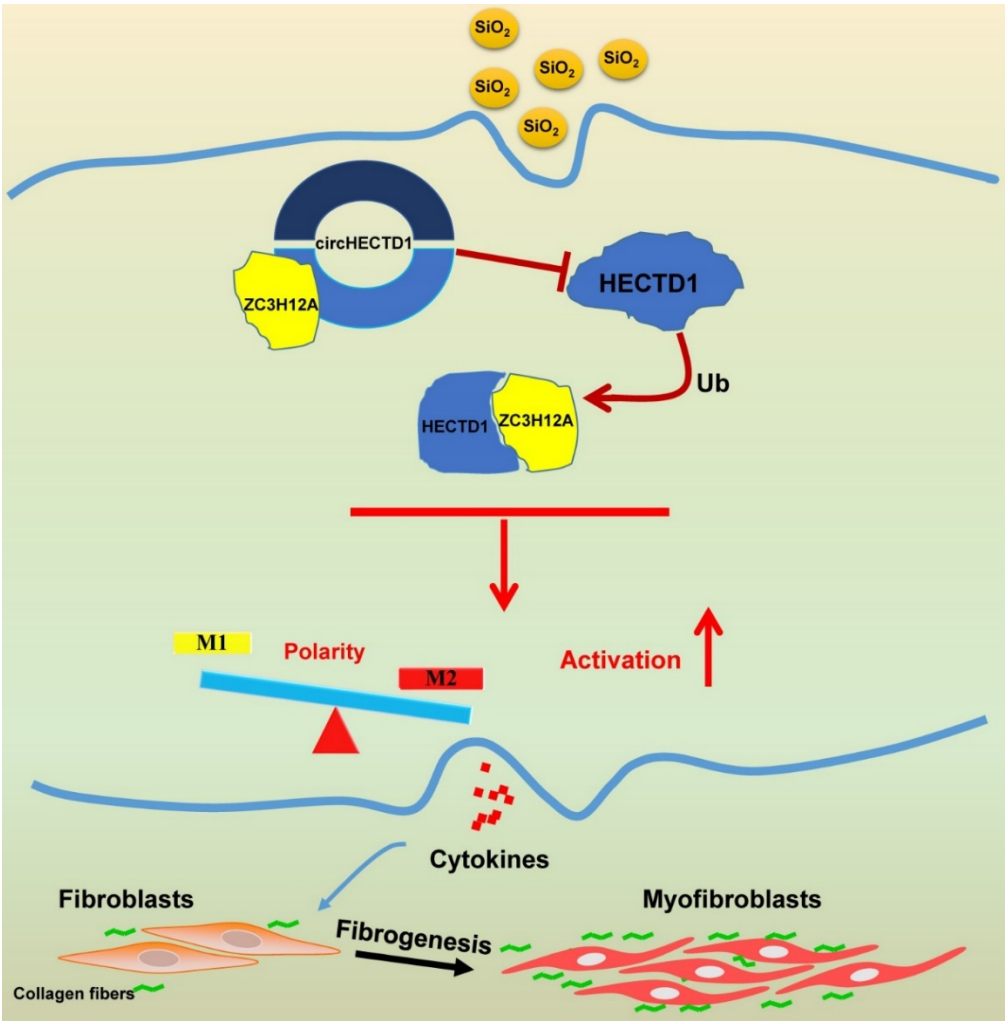


**Figure 10. Schematic diagram showing the mechanisms through which circHECTD1/HECTD1 in macrophages mediate silica-induced pulmonary fibrosis** circHECTD1 expression was decreased in macrophages exposed to $SiO_2$, leading to a subsequent increase in HECTD1 expression. The interactions between circHECTD1 and ZC3H12A and between HECTD1 and ZC3H12A might be involved in the balance of M1/M2 macrophages and thereby in the promotion of macrophage apoptosis. Macrophage apoptosis and activation resulted in overproduction of profibrogenic cytokines by macrophages. Fibroblasts responding to these cytokines differentiated into myofibroblasts, which showed enhanced proliferation and migration capacities as well as increased collagen synthesis.

## Competing Interests

The authors have declared that no competing interest exists.

## References

1. Steenland K, Ward E. Silica: a lung carcinogen. CA Cancer J Clin. 2014; 64: 63-9.
2. Verma DK, Ritchie AC, Muir DC. Dust content of lungs and its relationships to pathology, radiology and occupational exposure in Ontario hardrock miners. Am J Ind Med. 2008; 51: 524-31.
3. Leung CC, Yu IT, Chen W. Silicosis. Lancet. 2012; 379: 2008-18.
4. Tse LA, Li ZM, Wong TW, et al. High prevalence of accelerated silicosis among gold miners in Jiangxi, China. Am J Ind Med. 2007; 50: 876-80.
5. Mir SU, Jin L, Craven RJ. Neutrophil gelatinase-associated lipocalin (NGAL) expression is dependent on the tumor-associated sigma-2 receptor S2RPgrmc1. J Biol Chem. 2012; 287: 14494-501.
6. Wang K, Gan T-Y, Li N, et al. Circular RNA mediates cardiomyocyte death via miRNA-dependent upregulation of MTP18 expression. Cell Death Differ. 2017; 24: 1111-20.
7. Wu W, Shi SQ, Huang HJ, et al. Changes in PGRMC1, a potential progesterone receptor, in human myometrium during pregnancy and labour at term and preterm. Mol Hum Reprod. 2011; 17: 233-42.
8. Xu J, Zeng C, Chu W, et al. Identification of the PGRMC1 protein complex as the putative sigma-2 receptor binding site. Nat Commun. 2011; 2: 380.
9. Chen L, Zhang S, Wu J, et al. circRNA_100290 plays a role in oral cancer by functioning as a sponge of the miR-29 family. Oncogene. 2017; 36: 4551-61.

10. Zachariades E, Foster H, Goumenou A, et al. Expression of membrane and nuclear progesterone receptors in two human placental choriocarcinoma cell lines (JEG-3 and BeWo): effects of syncytialization. Int J Mol Med. 2011; 27: 767-74.
11. Memczak S, Jens M, Elefsinioti A, et al. Circular RNAs are a large class of animal RNAs with regulatory potency. Nature. 2013; 495: 333-8.
12. Zhang Y, Zhang XO, Chen T, et al. Circular intronic long noncoding RNAs. Mol Cell. 2013; 51: 792-806.
13. Ashwal-Fluss R, Meyer M, Pamudurti NR, et al. circRNA biogenesis competes with pre-mRNA splicing. Mol Cell. 2014; 56: 55-66.
14. Ruan X, Schneck H, Schultz S, et al. Nomegestrol acetate sequentially or continuously combined to estradiol did not negatively affect membrane-receptor associated progestogenic effects in human breast cancer cells. Gynecol Endocrinol. 2012; 28: 863-6.
15. Chao J, Wang X, Zhang Y, et al. Role of MCPIP1 in the endothelial-mesenchymal transition induced by silica. Cell Physiol Biochem. 2016; 40: 309-25.
16. Wessel L, Olbrich L, Brand-Saberi B, et al. New aspects of progesterone interactions with the actin cytoskeleton and neurosteroidogenesis in the cerebellum and the neuronal growth cone. J Histochem Cytochem. 2014; 62: 835-45.
17. Liu H, Fang S, Wang W, et al. Macrophage-derived MCPIP1 mediates silica-induced pulmonary fibrosis via autophagy. Part Fibre Toxicol. 2016; 13: 55.
18. Szczesna-Skorupa E, Kemper B. Progesterone receptor membrane component 1 inhibits the activity of drug-metabolizing cytochromes P450 and binds to cytochrome P450 reductase. Mol Pharmacol. 2011; 79: 340-50.
19. Chao J, Dai X, Pena T, et al. MCPIP1 regulates fibroblast migration in 3-D collagen matrices downstream of MAP kinases and NF-kappaB. J Invest Dermatol. 2015; 135: 2944-54.
20. Liu H, Dai X, Cheng Y, et al. MCPIP1 mediates silica-induced cell migration in human pulmonary fibroblasts. Am J Physiol Lung Cell Mol Physiol. 2016; 310: L121-32.
21. Zachariades E, Mparmpakas D, Thomas P, et al. Crucial cross-talk of interleukin-1beta and progesterone in human choriocarcinoma. Int J Oncol. 2012; 40: 1358-64.
22. Gordon S, Martinez FO. Alternative activation of macrophages: mechanism and functions. Immunity. 2010; 32: 593-604.
23. Whyte CS, Bishop ET, Ruckerl D, et al. Suppressor of cytokine signaling (SOCS)1 is a key determinant of differential macrophage activation and function. J Leukoc Biol. 2011; 90: 845-54.
24. Chhor V, Le Charpentier T, Lebon S, et al. Characterization of phenotype markers and neuronotoxic potential of polarised primary microglia in vitro. Brain Behav Immun. 2013; 32: 70-85.
25. Wang X, Zhang Y, Zhang W, et al. MCPIP1 regulates alveolar macrophage apoptosis and pulmonary fibroblast activation after in vitro exposure to silica. Toxicol Sci. 2016; 151: 126-38.
26. Ahmed IS, Chamberlain C, Craven RJ. S2R(Pgrmc1): the cytochrome-related sigma-2 receptor that regulates lipid and drug metabolism and hormone signaling. Expert Opin Drug Metab Toxicol. 2012; 8: 361-70.
27. Wilusz JE, Sharp PA. Molecular biology. A circuitous route to noncoding RNA. Science. 2013; 340: 440-1.
28. Sarkar AA, Zohn IE. Hectd1 regulates intracellular localization and secretion of Hsp90 to control cellular behavior of the cranial mesenchyme. J Cell Biol. 2012; 196: 789-800.
29. Wendler A, Albrecht C, Wehling M. Nongenomic actions of aldosterone and progesterone revisited. Steroids. 2012; 77: 1002-6.
30. Madri JA, Furthmayr H. Collagen polymorphism in the lung. An immunochemical study of pulmonary fibrosis. Hum Pathol. 1980; 11: 353-66.
31. Wang W, Liu H, Dai X, et al. p53/PUMA expression in human pulmonary fibroblasts mediates cell activation and migration in silicosis. Sci Rep. 2015; 5: 16900.
32. du Bois RM. The alveolar macrophage. Thorax. 1985; 40: 321-7.
33. Zhao MM, Cui JZ, Cui Y, et al. Therapeutic effect of exogenous bone marrowderived mesenchymal stem cell transplantation on silicosis via paracrine mechanisms in rats. Mol Med Rep. 2013; 8: 741-6.
34. Shearer JD, Richards JR, Mills CD, et al. Differential regulation of macrophage arginine metabolism: a proposed role in wound healing. Am J Physiol. 1997; 272: E181-90.
35. MacMicking J, Xie QW, Nathan C. Nitric oxide and macrophage function. Annu Rev Immunol. 1997; 15: 323-50.
36. Gogiraju R, Xu X, Bochenek ML, et al. Endothelial p53 deletion improves angiogenesis and prevents cardiac fibrosis and heart failure induced by pressure overload in mice. J Am Heart Assoc. 2015; 4: e001770.
37. Boeckel JN, Jae N, Heumuller AW, et al. Identification and characterization of hypoxia-regulated endothelial circular RNA. Circ Res. 2015; 117: 884-90.
38. Yin TP, Cai L, Xing Y, et al. Alkaloids with antioxidant activities from Aconitum handelianum. J Asian Nat Prod Res. 2016; 18: 603-10.
39. Zheng Q, Bao C, Guo W, et al. Circular RNA profiling reveals an abundant circHIPK3 that regulates cell growth by sponging multiple miRNAs. Nat Commun. 2016; 7: 11215.
40. Deng S, Huang C. E3 ubiquitin ligases in regulating stress fiber, lamellipodium, and focal adhesion dynamics. Cell Adh Migr. 2014; 8: 49-54.
41. Piguet PF, Collart MA, Grau GE, et al. Requirement of tumour necrosis factor for development of silica-induced pulmonary fibrosis. Nature. 1990; 344: 245-7.
42. Moore BB, Peters-Golden M, Christensen PJ, et al. Alveolar epithelial cell inhibition of fibroblast proliferation is regulated by MCP-1/CCR2 and mediated by PGE2. Am J Physiol Lung Cell Mol Physiol. 2003; 284: L342-9.
43. Rao KM, Porter DW, Meighan T, et al. The sources of inflammatory mediators in the lung after silica exposure. Environ Health Perspect. 2004; 112: 1679-86.
44. Zohn IE, Anderson KV, Niswander L. The Hectd1 ubiquitin ligase is required for development of the head mesenchyme and neural tube closure. Dev Biol. 2007; 306: 208-21.
45. Li X, Zhou Q, Sunkara M, et al. Ubiquitylation of phosphatidylinositol 4-phosphate 5-kinase type I gamma by HECTD1 regulates focal adhesion dynamics and cell migration. J Cell Sci. 2013; 126: 2617-28.
46. Tran H, Bustos D, Yeh R, et al. HectD1 E3 ligase modifies adenomatous polyposis coli (APC) with polyubiquitin to promote the APC-axin interaction. J Biol Chem. 2013; 288: 3753-67.
47. Del Valle PR, Milani C, Brentani MM, et al. Transcriptional profile of fibroblasts obtained from the primary site, lymph node and bone marrow of breast cancer patients. Genet Mol Biol. 2014; 37: 480-9.
48. Neubauer H, Chen R, Schneck H, et al. New insight on a possible mechanism of progestogens in terms of breast cancer risk. Horm Mol Biol Clin Investig. 2011; 6: 185-92.
49. Carpenter S, Ricci EP, Mercier BC, et al. Post-transcriptional regulation of gene expression in innate immunity. Nat Rev Immunol. 2014; 14: 361-76.
50. Bermejo-Alvarez P, Rizos D, Lonergan P, et al. Transcriptional sexual dimorphism in elongating bovine embryos: implications for XCI and sex determination genes. Reproduction. 2011; 141: 801-8.